Influence of a-Si:H/ITO interface properties on performance of heterojunction solar cells

Raphaël Lachaume, Wilfried Favre, Pascal Scheiblin, Xavier Garros, Nathalie Nguyen, Jean Coignus, Delfina Munoz, Gilles Reimbold

Available online at www.sciencedirect.com

ScienceDirect

Energy Procedia 38 (2013) 770 – 776

Energy Procedia

SiliconPV: March 25-27, 2013, Hamelin, Germany

Influence of a-Si:H/ITO interface properties on performance of heterojunction solar cells

Raphaël Lachaume[a,*], Wilfried Favre[b], Pascal Scheiblin[a], Xavier Garros[a], Nathalie Nguyen[b], Jean Coignus[b], Delfina Munoz[b], Gilles Reimbold[a]

[a]*CEA, LETI, MINATEC Campus, 17 rue des Martyrs, 38054 GRENOBLE Cedex 9, France*
[b]*CEA, INES RDI, 50 avenue du Lac Léman - Savoie Technolac - BP332, 73377 Le-Bourget-du-Lac, France*

Abstract

In this study, we focus on the influence of the contact properties between Indium Tin oxide (ITO) and hydrogenated amorphous Silicon (a-Si:H) on the performance of a-Si:H/c-Si HeteroJunction (HJ) solar cells. We experimentally found that an increase of the (p) a-Si:H layer thickness can improve the open-circuit voltage (Voc) but also and especially the Fill-Factor (FF) of the cell. Thanks to simulation we propose an explanation of this unexpected increase. The deposition of ITO with low effective workfunction on (p) a-Si:H actually leads to a depletion of the emitter of the cell, which results in an increase of its effective activation energy and of its resistance affecting Voc and FF. Thanks to this new insight we give guidelines which can help to further optimize the HJ front stack.

Keywords: heterojunction solar cells ; transparent conductive oxide ; indium tin oxide ; hydrogenated amorphous silicon ; contact ; work function ; simulation ; optimization

1. Introduction

The interest for hydrogenated amorphous silicon (a-Si:H) / crystalline silicon (c-Si) HeteroJunctions (HJ) solar cells arises from their high efficiencies (>20%) on large areas combined to an industrialization-ready fabrication process [1]. The performance of the HJ cell depicted in Fig. 1 strongly depends on the doping concentration, the bulk defect density and the respective thicknesses of (p) a-Si:H/ (i) a-Si:H layers which form the emitter of the cell. Indeed, modifying their properties affects both charge carrier transport at the junction (recombination, field effect) and photogeneration [2-4]. Furthermore, transparent

* Corresponding author. Tel.: +33-438-781-844; fax: +33-438-785-140
E-mail address: raphael.lachaume@cea.fr.

doi:10.1016/j.egypro.2013.07.345

conductive oxide (TCO) electrical (mainly its effective work function (EWF) and conductivity) and optical (transparency, absorbance) properties also have to be considered for a full optimization of the emitter [2, 5, 6]. Theoretical calculations have recently investigated the role played by the ITO/(p)a-Si :H on HET solar cells performance and especially on the Voc [7]. This paper will address the impact of ITO/(p) a-Si:H interface properties on the cell performance focusing on FF. Experimental optimization of FF is first done by changing the a-Si:H emitter thicknesses. HJ cells are fabricated on randomly textured n-type FZ c-Si wafers (104cm^2, 180µm; 1-5Ohm.cm) [8]. Then simulations are provided to explain the experimental results as well as to give general guidelines for further HJ cell optimization.

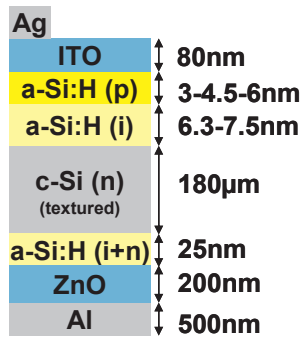

Fig. 1. Conventional HJ structure used in this study. Texturation of the fabricated solar cells is not represented.

2. Modeling

Solar cell characteristics have been modeled using a 2D finite elements simulation tool [9]. To simplify the analysis, simulation has been made in 1D mode neglecting both lateral transport and texturation. Electrical parameters for a-Si:H and c-Si were chosen in agreement with literature values [10]. Particularly, doping of a-Si:H layers has been calibrated by tuning dopant/bulk-defects ratio to fit the measured conductivity versus inverse temperature curves [4]. The latter provide us with the layer activation energy Ea defined by the difference between the bulk Fermi level E_F and the valence band energy E_V [11]. These Ea measurements are also used to deduce the work function of the p-aSi layer ($WF^{p\text{-}aSi}$) given here by $WF^{p\text{-}aSi}=E_F{}^{p\text{-}aSi}=\chi^{aSi}+Eg^{aSi}-Ea^{p\text{-}aSi}$ where χ^{aSi}=3.85eV is the electronic affinity with respect to the vacuum level and Eg^{aSi}=1.7eV is the a-Si:H bandgap. Moreover a-Si:H thicknesses used in the simulation correspond to the thicknesses on textured substrates, which are obtained by dividing the thickness on polished wafers, due to geometrical effects, by a factor of 1.6 for a-Si:H and 1.2 for TCOs [3]. Note that layers are considered to be uniform, i.e. the composition of the a-Si:H layers are thickness independent. Only simulation results for the case i-layer=6.3nm are presented in the following study. Transfer matrix method is used to calculate photogeneration thanks to optical indices of the various layers, directly extracted from ellipsometry measurements. ITO is considered as a Schottky metal contact with a fixed effective work function (EWF). In this simulation study, EWF is varying from below to above the Fermi Level of the p-aSi layer estimated to ~5.2eV. It is in agreement with generally measured values for ITO EWF in literature, which can vary from 4.1eV to 5.53eV [12]. Infinite surface recombination is also considered at the ITO/a-Si:H interface, assuming that either a barrier height reduction due to high concentration of surface states or sufficient tunneling mechanisms do not impede recombination between electrons in ITO and holes in the p-layer [6, 11]. In this way, simulation does

show the electrostatic effect of ITO EWF on the underlying layers and, hence, on the cell performance. Thermionic-field emission models included in the simulator are also used to simulate transport processes at the a-Si:H/c-Si interface [9]. The resistance of this interface potential barrier is denoted R^{int}. An external series resistance R^{ext} of 0.4Ω/cm2 is added to take into account the contribution of metallization in the total resistance of the cell.

3. Results and discussion

3.1. Experimental results

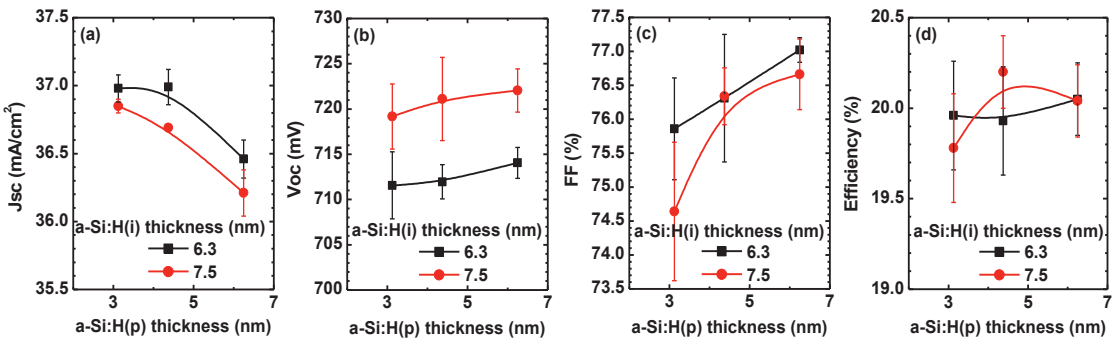

Fig. 2. J(V) measurement parameters of our HJ cells versus p-layer thickness for 6.3nm and 7.5nm of i-layer. Measurements were made under AM1.5 conditions using an AESCUSOFT I-V tool.

Fig. 2 shows the main electrical features of our HJ cells for different thicknesses of the a-Si:H emitter. For each thickness, three cells were fabricated. The corresponding mean value and standard deviation of the parameters are then reported in the graphs. Firstly, we notice that Jsc decreases with increasing a-Si:H thickness (see Fig. 2(a)). This was expected and explained by parasitic optical absorption of the a-Si:H emitter [3]. Secondly, we notice that the Voc increases with increasing i-layer thickness independently of the p-layer (see Fig. 2(b)). We attribute this to a better passivation of the a-Si:H/c-Si interface as suggested by many authors [1]. At this stage it is worth noticing that this gain in Voc was rather expected. But what is most surprising is the FF increase of ~1.5% observed for both i-layer thicknesses in Fig. 2(c). The reason for this FF increase remains unclear [3]. To explain it, we have extracted the total series resistance Rs from J(V) curves under illumination by linear regression around Voc. Results are shown in Fig. 3. Clearly, the FF variations appear correlated to Rs for all the different measured cells. Therefore, understanding the Rs variations allows to explain this unexpected FF behavior.

In fact, we would have expected 2 possible scenarios. The first one is that the resistance of the emitter is negligible compared to the resistances related to the other layers and interfaces. In this case, transport through this layer would not be a limiting factor and, in turn, no significant variation of FF should be observed. The second scenario is that the resistance of the p-layer is not anymore negligible compared to the other resistances. Therefore increasing the p-aSi thickness would come with an increase of its associated resistance affecting significantly the total Rs of the cell, and in turn, FF should decrease. None of these 2 scenarios fit with the observed experimental variations of Fig. 2(c) and 3(b). Hence, in the following part, we propose a third scenario thanks to simulation in order to explain this FF increase with p-layer thickness.

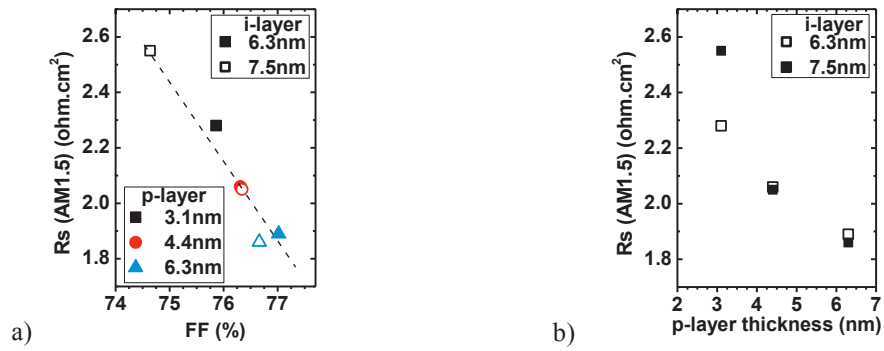

Fig. 3. Cell series resistance (Rs) under AM1.5 illumination versus FF (a) and versus p-layer thickness (b). Rs is extracted from J(V) curves by linear regression around Voc. Only the mean value is given for Rs and FF for the sake of clarity. Open (full) symbols refer to 7.5nm (6.3nm) of i-layer.

3.2. Simulation results

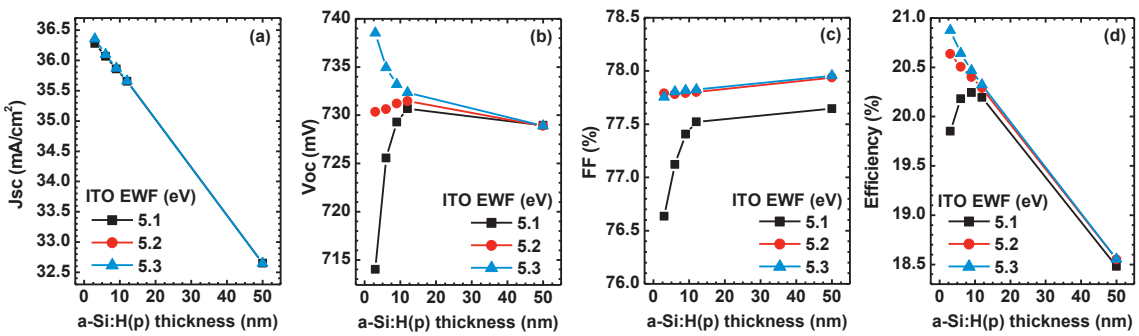

Fig. 4. J(V) simulated parameters of our HJ cells versus p-layer thickness for a 6.3nm i-layer. ITO EWF is varying from 5.1eV to 5.3eV. It lies above or below the Fermi level in the p-aSi layer estimated to ~5.2eV.

Fig.4 reports the J(V) parameters of the cell, which have been simulated for different thicknesses of the p-aSi layer from 3nm to 50nm.The extreme case $t^{a\text{-}Si}$=50nm is only used, in the following text, to show the saturation effects of the cell performance for thick layers but does not correspond to an experimental case. We successfully reproduce, by simulation, the experimental variations of Jsc, Voc and FF with the p-layer thickness with ITO EWF=5.1eV. The decrease of Jsc with increasing p-aSi thickness is well known while the Voc and FF increase is not trivial. It cannot be explained without taking into account the electrostatic effect of ITO on top. Actually 3 cases can be considered depending on the relative position of the ITO EWF with respect to the work function of the bulk p-aSi layer estimated here to ~5.2eV. Basically when a contact is formed between this layer and an electrode with a given work function, a charge transfer occurs to reach the electrostatic equilibrium. This induces the formation of either a depletion or an accumulation region within the p-layer depending on the ITO EWF. This also results in a local band bending and in a variation of the effective Ea of the a-Si:H layer, and, in turn, comes with a variation of the internal voltage of the cell Vbi visible on Voc variations (see Fig. 4(b)).

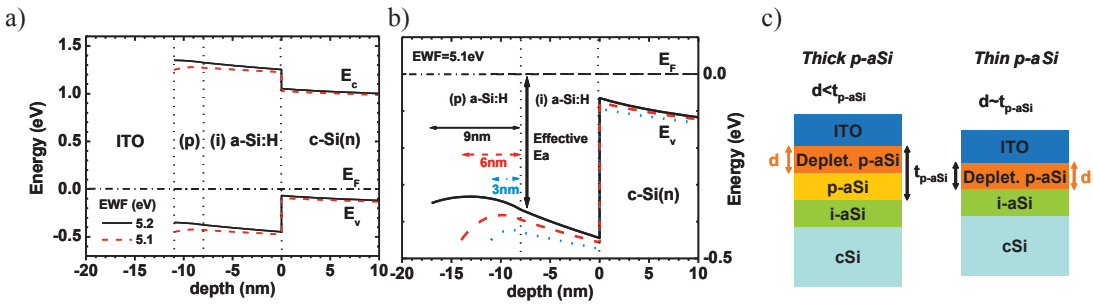

Fig. 5. Simulated front band diagrams in dark equilibrium versus depth for (a) ITO EWF=5.2eV and EWF=5.1eV and (b) for different p-layer thicknesses in case EWF=5.1eV. (c) Schematics representing the depletion occurring at ITO/p-aSi interface for a thick and a thin layer.

For ITO EWF=5.1eV, which corresponds to the real case of Fig. 2, the a-Si:H layer is depleted along a given extent d as illustrated in Fig. 5 (c). In addition, bands are bending downwards resulting in an increase of the effective Ea of the emitter (see Fig. 5 (a) and (b)). For thin (p) a-Si:H layer $t_{p\text{-}aSi}$ ~3nm, the whole layer is depleted d~$t_{p\text{-}aSi}$ and the effective Ea=E_F^{aSi}-E_V^{aSi} is increased in both doped and intrinsic a-Si:H layers. The corresponding resistivities ρ_i and ρ_p become so important that the total resistance of the emitter R^{aSi} given by $\rho_i.t^{i\text{-}aSi}+\rho_p.t^{p\text{-}aSi}$ is increased even though the emitter thickness is decreased. For thick (p) a-Si:H layers $t_{p\text{-}aSi}$ >9nm, the p-layer is only partially depleted d<$t^{p\text{-}aSi}$. This allows the (i+p) stack to recover its intrinsic properties over a significant depth t^{aSi} –d. The effective Ea in this region reaches the respective bulk values for single p-doped and intrinsic aSi. The resistivity ρ_i and ρ_p are then much lower than for thin p-layers as well as R^{aSi} even though $t^{p\text{-}aSi}$ is thicker. All these phenomena are clearly illustrated in Fig. 6(a) which shows the respective resistances of both (i) and (p) aSi layers as well as the effective Ea for different p-aSi thicknesses.

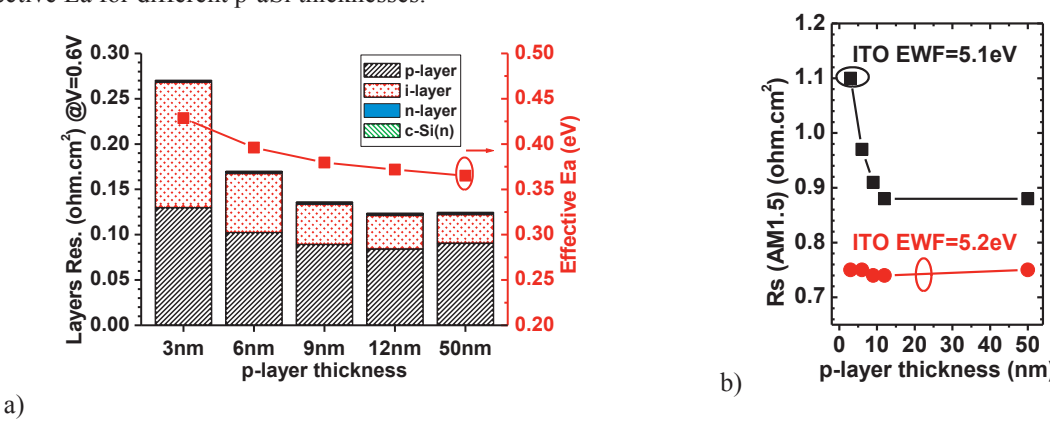

Fig. 6. (a) Detailed layer resistances in the simulated device extracted at the maximum power point V~0.6V and effective Ea showed for different p-layer thicknesses and for ITO EWF=5.1eV. (b) Total Rs of the simulated cell, extracted from simulated J(V) curves by linear regression around Voc.

Moreover, Rs has also been extracted from simulated J(V) curves around Voc to evaluate the contribution of the emitter layer resistance R^{aSi} to the total cell resistance Rs=R^{aSi}+R^{ext}+R^{int}. Results are plotted against p-layer thickness on Fig. 6(b). We notice that Rs increases with decreasing p-aSi thickness

exactly as R^{aSi} (see Fig 6(a)). This is also perfectly consistent with the experimental results shown in Fig. 3(b). These variations of Rs have a strong impact on FF due to the strong correlation between Rs and FF (see Fig. 3(a)). Fig. 4(c) shows that FF drops of nearly 1% when p-aSi is reduced from 12nm to 3nm. Again we reproduce pretty well the experimental decrease of FF ~1.5% with p-aSi thickness observed in Fig. 2(c). Moreover we foresee by simulation that, when the p-aSi layer becomes thick, Voc and FF saturate while Jsc continues to decrease. This explains why the compromise in term of efficiency is found around $t^{p\text{-}aSi}$=9nm for ITO EWF=5.1eV. Another way to improve the cell performance is to achieve a high effective work function for the TCO, in this case above 5.3eV. In this latter ideal case, holes are accumulated near the contact, resulting in an improvement of the resistivity of the a-Si:H emitter and, in turn, the FF of the cell is not affected as seen in Fig. 4(c). This time, p-layer thickness may successfully be reduced to gain in Jsc without loosing FF and, to finally gain in efficiency.

4. Conclusion

The increase of FF and Voc with increasing p-layer thickness has been explained thanks to simulation. In case the ITO effective work function is lower than the p-aSi layer one, a depletion of the p-layer occurs, which increases both the effective activation energy and the resistivity of the a-Si:H emitter. This effect is critical when the p-layer is decreased. The emitter resistance increases leading to an increased cell Rs and hence results in a FF drop. Optimization of ITO work function on a-Si:H is thus of crucial importance to be able to improve HJ cell performance.

Acknowledgements

The author would like to acknowledge the HET team for providing characterization data.

References

[1] De Wolf, S., Descoeudres, A., Holman, Z.C., Ballif, C. High-efficiency Silicon Heterojunction Solar Cells: A Review. *green* 2012; **2**: 7-24.

[2] Fujiwara, H., Kondo, M.. Effects of a - Si:H layer thicknesses on the performance of a - Si:H/c - Si heterojunction solar cells. *Journal of Applied Physics* 2007; **101**: 054516 – 054525.

[3] Holman, Z.C., Descoeudres, A., Barraud, L., Fernandez, F.Z., Seif, J.P., De Wolf, S. et al., Current Losses at the Front of Silicon Heterojunction Solar Cells. *IEEE Journal of Photovoltaics* 2012; **2**: 7–15.

[4] Lachaume, R., Coignus, J., Garros, X., Scheiblin, P., Munoz, D., Reimbold, G., Impact of bulk defects in hydrogenated amorphous Si layers on performance of high efficiency HeteroJunctions solar cells assessed by 2D modeling, in: *proceedings of the 2012 13th International Conference on Ultimate Integration on Silicon (ULIS)*, p. 97–100.

[5] Centurioni, E., Iencinella, D., Role of front contact work function on amorphous silicon/crystalline silicon heterojunction solar cell performance. *IEEE Electron Device Letters* 2003; **24**: 177–179.

[6] Kanevce, A., Metzger, W.K., The role of amorphous silicon and tunneling in heterojunction with intrinsic thin layer (HIT) solar cells. *Journal of Applied Physics* 2009; **105**: 094507–094514.

[7] Varache, R., Kleider, J.P., Gueunier-Farret, M.E., Korte, L., Silicon heterojunction solar cells: Optimization of emitter and contact properties from analytical calculation and numerical simulation. *Materials Science and Engineering: B* 2013, **178**: 593-598

[8] Muñoz, D., Ozanne, A.S., Harrison, S., Danel, A., Souche, F., Denis et al., Towards high efficiency on full wafer a-Si:H/c-Si heterojunction solar cells: 19.6% on 148cm2, in: *proceedings of the 2010 35th IEEE PVSC*, p. 39 –43.

[9] SILVACO ATLAS User's Manual; 2012.

[10] Hernández-Como, N., Morales-Acevedo, A., Simulation of hetero-junction silicon solar cells with AMPS-1D. *Solar Energy Materials and Solar Cells* 2010; **94**: 62–67.

[11] Street R. A., *Hydrogenated Amorphous Silicon*, Cambridge University Press; 1991.

[12] Park, Y., Choong, V., Gao, Y., Hsieh, B.R., Tang, C.W. Work function of indium tin oxide transparent conductor measured by photoelectron spectroscopy. *Applied Physics Letters* 1996; **68**: 2699–2701.